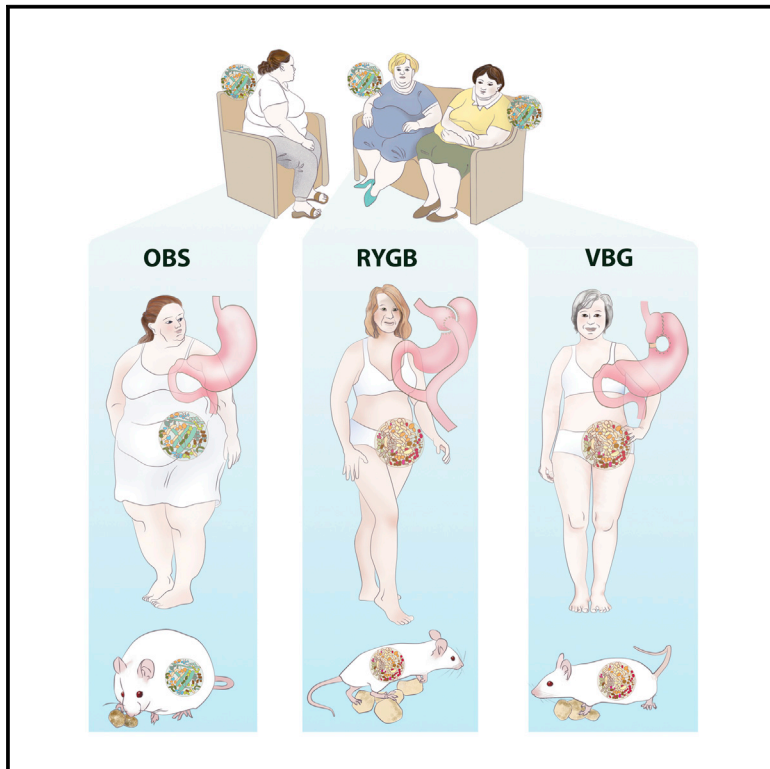# Roux-en-Y Gastric Bypass and Vertical Banded Gastroplasty Induce Long-Term Changes on the Human Gut Microbiome Contributing to Fat Mass Regulation

Graphical Abstract

Authors

Valentina Tremaroli, Fredrik Karlsson, Malin Werling, ..., Carel W. le Roux, Jens Nielsen, Fredrik Bäckhed

Correspondence

Fredrik.Backhed@wlab.gu.se

In Brief

Bariatric surgery durably alters the human gut microbiome. Here, Tremaroli et al. demonstrate that two types of bariatric surgery, Roux-en-Y gastric bypass and vertical banded gastroplasty, produce long-term alterations of the gut microbiome independently of BMI and that these alterations modulate host metabolism and fat mass deposition.

Highlights

- RYGB and VBG induce long-term alterations in the human gut microbiome

- The changes in the microbiome do not depend on BMI

- RYGB and VBG have different effects on bile acid and TMAO metabolism

- The surgically altered microbiome contributes to fat mass regulation

CrossMark

CellPress

Roux-en-Y Gastric Bypass and Vertical Banded Gastroplasty Induce Long-Term Changes on the Human Gut Microbiome Contributing to Fat Mass Regulation

Valentina Tremaroli,[1,6] Fredrik Karlsson,[2,6,7] Malin Werling,[3] Marcus Ståhlman,[1] Petia Kovatcheva-Datchary,[1] Torsten Olbers,[3] Lars Fändriks,[3] Carel W. le Roux,[3,4] Jens Nielsen,[2] and Fredrik Bäckhed[1,5,*]

[1]The Wallenberg Laboratory and Sahlgrenska Center for Cardiovascular and Metabolic Research, Department of Molecular and Clinical Medicine, Institute of Medicine, University of Gothenburg, SE-413 45 Gothenburg, Sweden
[2]Department of Biology and Biological Engineering, Chalmers University of Technology, SE-412 96 Gothenburg, Sweden
[3]Department of Gastrosurgical Research and Education, Sahlgrenska Academy, University of Gothenburg, Sahlgrenska University Hospital/Sahlgrenska, SE-413 45 Gothenburg, Sweden
[4]Diabetes Complications Research Centre, UCD Conway Institute, School of Medicine and Medical Sciences, University College Dublin, Ireland
[5]Novo Nordisk Foundation Center for Basic Metabolic Research, Section for Metabolic Receptology and Enteroendocrinology, Faculty of Health Sciences, University of Copenhagen, Copenhagen, DK-2200, Denmark
[6]Co-first author
[7]Present address: Metabogen AB, 411 26 Gothenburg, Sweden
*Correspondence: Fredrik.Backhed@wlab.gu.se
http://dx.doi.org/10.1016/j.cmet.2015.07.009

SUMMARY

Bariatric surgery is currently the most effective procedure for the treatment of obesity. Given the role of the gut microbiota in regulating host metabolism and adiposity, we investigated the long-term effects of bariatric surgery on the microbiome of patients randomized to Roux-en-Y gastric bypass or vertical banded gastroplasty and matched for weight and fat mass loss. The two surgical procedures induced similar and durable changes on the gut microbiome that were not dependent on body mass index and resulted in altered levels of fecal and circulating metabolites compared with obese controls. By colonizing germ-free mice with stools from the patients, we demonstrated that the surgically altered microbiota promoted reduced fat deposition in recipient mice. These mice also had a lower respiratory quotient, indicating decreased utilization of carbohydrates as fuel. Our results suggest that the gut microbiota may play a direct role in the reduction of adiposity observed after bariatric surgery.

INTRODUCTION

The prevalence of obesity and its metabolic comorbidities, such as type 2 diabetes and cardiovascular disease, is on the rise worldwide. Although a number of genetic and environmental factors have been identified, the mechanisms responsible for excessive fat mass accumulation and development of obesity are not fully understood. Recent research shows that our intestinal microbes contribute to the regulation of energy homeostasis and fat storage and may play a role in obesity and its complications (Karlsson et al., 2013; Qin et al., 2012; Smith et al., 2013; Tremaroli and Bäckhed, 2012). Indeed, obesity has been associated with altered gut microbiota composition, reduced microbial diversity, and reduced gene richness (Le Chatelier et al., 2013; Ley et al., 2005; Turnbaugh et al., 2009). In addition, dietary weight loss interventions have been shown to increase gene richness of the microbiota and shift its composition toward that of lean individuals (Cotillard et al., 2013; Ley et al., 2006).

Bariatric surgery is currently the best treatment for sustained weight loss and reduction of obesity-related comorbidities (Sjöström et al., 2007, 2012). There are a number of bariatric surgery procedures, of which Roux-en-Y gastric bypass (RYGB) is considered one of the most effective, promoting both weight reduction and improvement of metabolism (Sjöström et al., 2007; Werling et al., 2013a). The underlying mechanisms have not been fully elucidated, but reduced food ingestion, changes in food preferences, increased satiety, release of satiety-promoting gut hormones (e.g., glucagon-like peptide 1 [GLP-1] and peptide YY [PYY]), increased gastric emptying, and a shift in bile acid metabolism together with an increased signaling through the bile acid nuclear receptor farnesoid X receptor (FXR) have all been suggested to play a role (le Roux and Bloom, 2005; Miras and le Roux, 2013; Ryan et al., 2014).

Recent work has also indicated that the gut microbiota may mediate some of the beneficial effects of bariatric surgery, and changes in the composition and diversity of the gut microbiota have been observed in the short term after RYGB in humans (Furet et al., 2010; Graessler et al., 2013; Kong et al., 2013; Zhang et al., 2009), as well as after vertical sleeve gastrectomy and RYGB in mice (Liou et al., 2013; Ryan et al., 2014). However, there are no long-term investigations of the stability of these changes or of the effects of different procedures on the human gut microbiota. Additionally, the causal link between the alterations to the microbiota and the reduction in adiposity observed
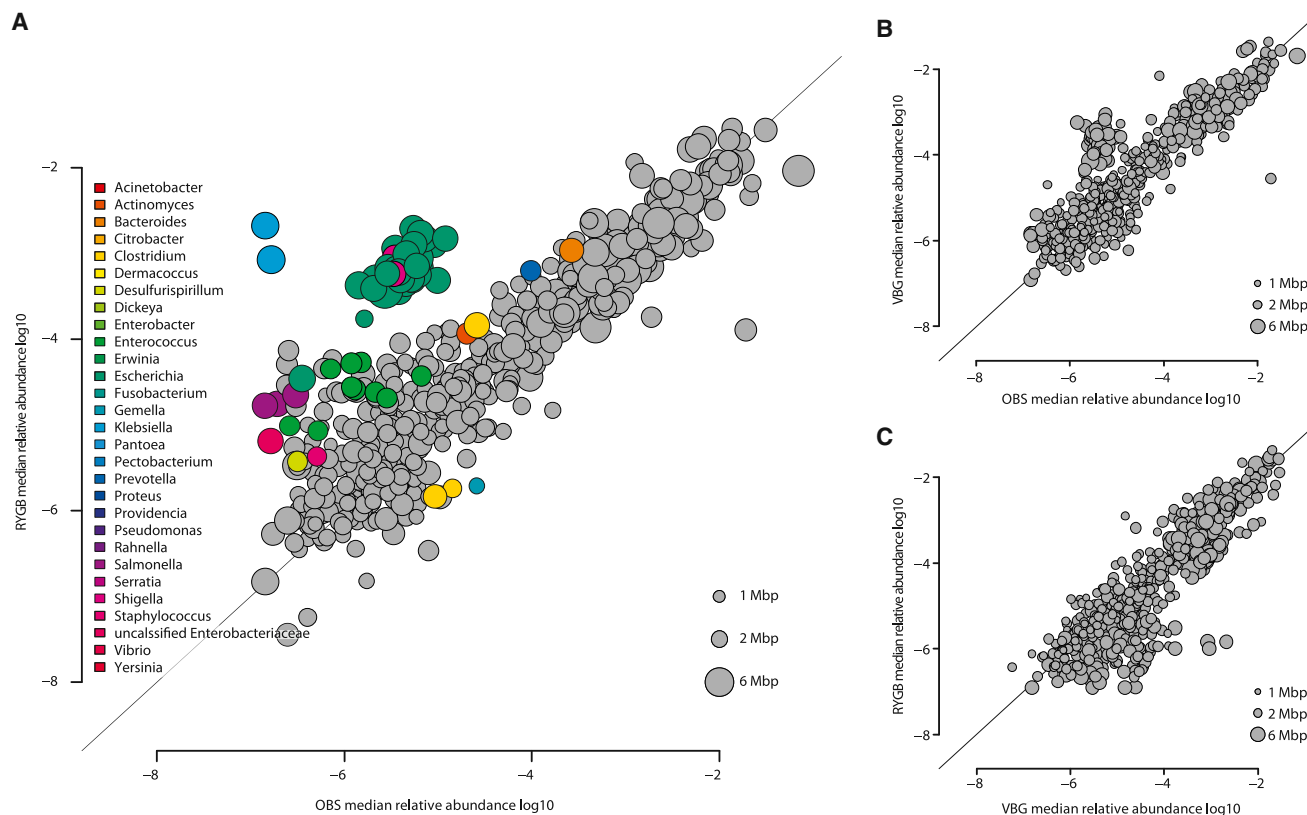
Figure 1. Long-term Effects of Bariatric Surgery on Gut Microbiota Composition
(A) Scatter plot of median species abundance in RYGB patients and severely obese subjects (OBS).
(B) Scatter plot of median species abundance in VBG patients and OBS subjects.
(C) Scatter plot of median species abundance in RYGB and VBG patients.
The genus affiliations of differentially abundant species are indicated by color (Adj. p < 0.05, Wilcoxon rank-sum test). See also Table S3.

after bariatric surgery has not been previously analyzed in humans.

Here we used shotgun sequencing of the human fecal metagenome to analyze the gut microbiota of weight-stable women 9 years after randomization to either RYGB or vertical banded gastroplasty (VBG) (Olbers et al., 2006) and matched for weight and fat mass loss. As a reference, we also analyzed the gut microbiota of two groups of non-operated women with body mass index (BMI) matched to the patients' pre-surgical BMI (OBS) and post-surgical BMI (Ob). We aimed to identify whether alterations in the gut microbiota observed previously in the short term remained stable over time and if RYGB and VBG induced specific alterations in the gut microbiome. Moreover, we investigated the causal link between the surgically altered human gut microbiota and adiposity phenotype by performing microbiota transplantations of human stools in germ-free (GF) mice.
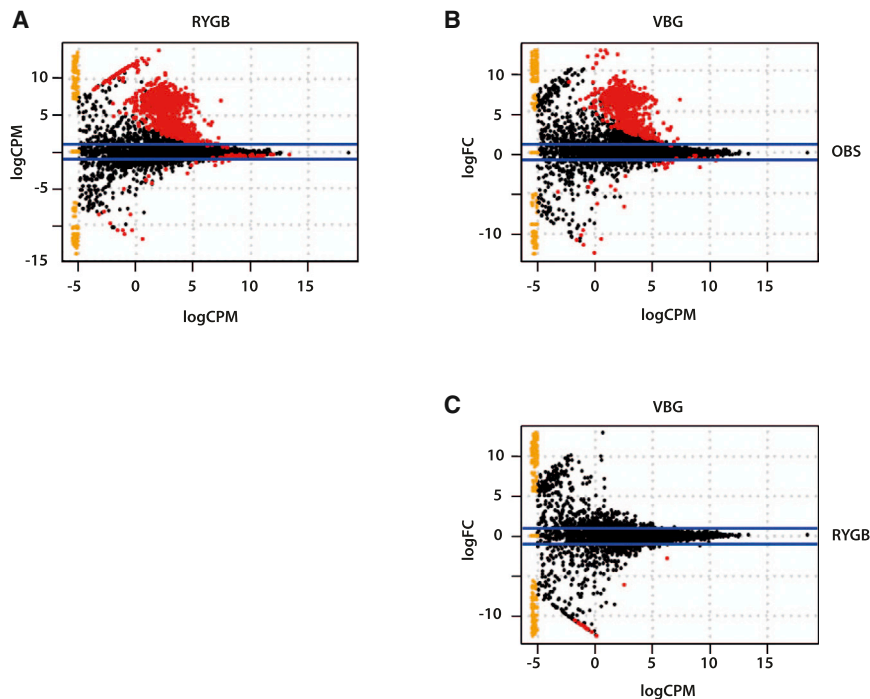
RESULTS AND DISCUSSION

Bariatric Surgery has Long-Term Effects on Gut Microbiota Composition

To investigate the long-term effects of bariatric surgery on the gut microbiota, we obtained fecal samples from 14 women 9.4 years after they were randomized to RYGB (n = 7) or VBG

(n = 7) (Olbers et al., 2006). These women were included in a recent study of the mechanisms underlying the maintenance of long-term weight loss (Werling et al., 2013b). RYGB and VBG patients were matched for pre- and post-operative weight, BMI, and body composition, and had thus experienced similar weight and fat mass loss. We also included fecal samples from seven non-operated women with severe obesity (OBS) and a BMI similar to the mean pre-surgical BMI of RYGB and VBG patients. Clinical and biometric measurements of these three groups of women are summarized in Table S1.

Genomic DNA was extracted from fecal samples using a repeated bead beating procedure (Salonen et al., 2010) and sequenced on Illumina HiSeq 2000. In total, we obtained 63 Gbp of paired-end reads, with an average of 3.0 ± 3.0 (SD) Gbp for each sample (Table S2). To determine the composition of the gut microbiota, we aligned high-quality Illumina reads devoid of human DNA to 2,382 reference genomes obtained from the National Center for Biological Information (NCBI) and the Human Microbiome Project (HMP) databases (http://hmpdacc.org) (Table S2) using methods from our MEDUSA platform (Karlsson et al., 2012; Karlsson et al., 2014).

We observed significant differences in microbiota composition for RYGB versus OBS samples, but not for VBG versus OBS or RYGB versus VBG (Figure 1; Table S3). The abundance of

Figure 2. Functional Differences in the Microbiomes of RYGB, VBG and OBS Subjects as Measured by the Abundance of KOs
(A) Comparison of RYGB versus OBS samples.
(B) Comparison of VBG versus OBS samples.
(C) Comparison of RYGB versus VBG samples.
Each spot represents a KO, and red spots represent KOs whose abundance is significantly different. FC, fold change; CPM, counts per million. See also Table S4 and Figures S1 and S2.

mechanisms common to the two surgical procedures might affect the composition of the gut microbiota. For example, increases in pH have been shown to promote the growth of *E. coli* in vitro (Duncan et al., 2009), and both RYGB and VBG are associated with reduced luminal exposure to gastric acidity.

Bariatric Surgery Has Long-Term Effects on the Genetic Content of the Gut Microbiota

To explore the genetic content of the gut microbiome after bariatric surgery, we aligned our reads to the MetaHIT human gut microbial gene catalog (Qin et al., 2010). We calculated the abundance of KEGG orthologs (KOs), and analyzed the abundance of KEGG pathways using the reporter features algorithm to obtain a global view of the changes (Oliveira et al., 2008; Patil and Nielsen, 2005).

We observed differences in the microbiome of operated and non-operated severely obese women (Figure 2; Table S4): 928 KOs were enriched and 60 were depleted in RYGB versus OBS samples (Figure 2A; Table S4), while 682 KOs were enriched and 33 were depleted in VBG versus OBS samples (Figure 2B; Table S4). However, only 17 KOs were differentially abundant between RYGB and VBG samples, all enriched in VBG (Figure 2C; Table S4).

The reporter pathways for phosphotransferase systems and fluorobenzoate degradation were enriched in RYGB versus OBS microbiomes, and the reporter pathways for flagellar assembly, sulfur relay system, glutathione metabolism, glyoxylate and dicarboxylate metabolism, ABC transporters (in particular for lysine/arginine/ornithine, histidine, and putrescine), and phenylalanine metabolism were enriched in VBG versus OBS samples (Table 1; Table S4). In addition, the reporter pathways for nitrogen metabolism, fatty acid metabolism, and two-component systems were enriched both in RYGB versus OBS and VBG versus OBS microbiomes (Tables 1 and S4).

Two-component systems are sensory systems that enable bacteria to sense and respond to changes in the surrounding environment (Mascher et al., 2006). We found that the two-component systems responding to nitrogen availability (*nifA*), phosphoglycerate transport (*pgtCAP*), and short-chain fatty acid (SCFA) metabolism (acetoacetate, *atoCE*) were specifically enriched in RYGB compared to OBS, while salt stress response and twitching motility were specifically enriched in VBG compared to OBS (Table S4). Two-component system genes

species belonging to 29 microbial genera differed significantly between RYGB and OBS samples (Figure 1A; Table S3); in particular, the levels of several species in the Gammaproteobacteria class were higher while the levels of three species in the Firmicutes phylum (*Clostridium difficile*, *Clostridium hiranonis*, and *Gemella sanguinis*) were lower in RYGB versus OBS samples (Table S3). At the genus level, several facultative anaerobes in the Proteobacteria (e.g., *Escherichia*, *Klebsiella*, and *Pseudomonas*) were present at increased relative abundance in RYGB (Table S3). We observed a different relative abundance for several species when comparing VBG with OBS samples, and RYGB with VBG samples, although the differences were not significant after correction for multiple testing (Table S3). *E. coli* tended to increase, while *Eubacterium rectale* and *Roseburia intestinalis* tended to decrease in VBG compared to OBS (Table S3). *Klebsiella* species tended to increase, while *Bifidobacterium* species tended to decrease in RYGB in comparison to VBG (Table S3).

These analyses demonstrated that women who have undergone RYGB had increased abundance of Proteobacteria in comparison to non-operated severely obese women. Proteobacteria are generally not considered to be beneficial due to their proinflammatory properties (Amar et al., 2011; Cani et al., 2007; Mukhopadhya et al., 2012). However, the RYGB and VBG patients in our study were not under inflammatory stress as determined by plasma CRP levels (Table S1). Moreover, our results are in agreement with previous findings showing an expansion of Proteobacteria shortly after RYGB, both in humans (Furet et al., 2010; Graessler et al., 2013; Kong et al., 2013; Zhang et al., 2009) and mice (Liou et al., 2013). Additionally, despite the obvious differences between the two surgical procedures (Olbers et al., 2006), we did not observe distinct microbiota profiles for RYGB and VBG patients. Although this result could be due to the small sample size of our cohort, it is also possible that other

Table 1. KEGG Pathways Enriched in the Gut Microbiomes of RYGB and VBG Patients in Comparison to OBS Women

RYGB Enriched Compared to OBS	VBG Enriched Compared to OBS
–	Flagellar assembly
–	Sulfur relay system
–	Glutathione metabolism
–	Glyoxylate and dicarboxylate metabolism
–	ABC transporters
–	Phenylalanine metabolism
Nitrogen metabolism	Nitrogen metabolism
Fatty acid metabolism	Fatty acid metabolism
Two-component system	Two-component system
Phosphotransferase system	–
Fluorobenzoate degradation	–

for response to antimicrobial peptides, outer membrane stress, and trimethylamine *N*-oxide (TMAO) were enriched in both RYGB and VBG compared to OBS microbiomes. Furthermore, the gene coding for TMAO reductase (*torA*, K07811), which is involved in the respiration of TMAO to TMA, was also enriched in both RYGB and VBG compared to OBS microbiomes (Table S4).

The increase in *tor* genes likely reflects the high levels of *E. coli* in both RYGB and VBG samples, as *E. coli* can use TMAO as a terminal electron acceptor (Barrett and Kwan, 1985). However, we observed increased plasma concentrations of TMAO only in RYGB and not in VBG women (Figure S1A); the levels of choline and betaine, known dietary precursors for TMA production by the gut microbiota, did not differ between the groups (Figures S1B and S1C). The increased levels of TMAO in RYGB samples might be the consequence of a less anaerobic metabolism in the RYGB intestine, which is supported by the broad increase of facultative anaerobes in RYGB microbiomes, and could occur due to the shortening of the small bowel. We speculate that TMAO could be produced in the intestine by oxidation of TMA catalyzed by TMA monooxygenase; this enzyme is present in bacteria such as *Pseudomonas* (Barrett and Kwan, 1985), which showed increased abundance in RYGB microbiomes.

These observations are of interest because high TMAO levels linked to TMA oxidation by the human hepatic flavin monooxygenase FMO3 have been associated with cardiovascular diseases (CVDs) (Tang et al., 2013; Wang et al., 2011), while it is known that RYGB is associated with a lower CVD risk (Sjöström et al., 2012).

Bariatric Surgery Has Long-Term Effects on Microbial Fermentation

The enrichment of KOs related to phosphoglycerate, acetoacetate, and SCFAs transporters and to phosphotransferase systems pointed to increased energy flux into sugar metabolism and glycolysis in RYGB microbiomes. By contrast, the enrichment of pathways for amino acid uptake and metabolism and for glyoxylate metabolism pointed to the utilization of amino acids and acetate for energy production by the VBG microbiome. As the fermentation activities of the gut microbiota

contribute to host nutrition and health (Flint et al., 2012), we functionally tested whether the differences in the microbiome resulted in altered microbial fermentation of carbohydrate and protein by measuring the levels of fecal SCFAs and branched-chain fatty acids (BCFAs). The SCFAs acetate, propionate, and butyrate were present in comparable proportions, but their concentrations tended to decrease in RYGB and VBG samples (Figures S2A–S2D), while the BCFAs isobutyrate and isovalerate, produced from the amino acids valine and leucine, respectively, either showed no change or a slight tendency to increase in RYGB and VBG samples (Figures S2E–S2G). As a result, we observed a decrease in the SCFA/BCFA ratio for bariatric surgery samples, which was significant for RYGB (Figure S2H). Importantly, total fiber intake did not differ, while protein intake decreased for RYGB and VBG women (Table S1), indicating that the lower SCFA/BCFA ratio was not a consequence of dietary consumption.

The similar SCFA/BCFA ratio and the analysis of pathways enriched in RYGB and VBG compared to OBS subjects reveal some common effects of the two bariatric surgery procedures and indicate altered intestinal fermentation shifted toward reduced production of SCFAs and increased amino acid fermentation after bariatric surgery. As the total fiber intake was similar for RYGB, VBG, and OBS patients, our results point to a diet-independent adaptation of the gut microbiota to bariatric surgery. In particular the decreased SCFAs levels in RYGB and VBG fecal samples also point to reduced energy harvest from the diet, as previously proposed (Turnbaugh et al., 2006).

Bariatric Surgery Has Long-Term Effects on Bile Acid Metabolism

Bile acids are cholesterol metabolites that facilitate the absorption of dietary fat and fat-soluble molecules and are now also recognized as regulators of energy metabolism through activation of the receptors TGR5 and FXR (Hylemon et al., 2009; Lefebvre et al., 2009). Increased circulating levels of primary and secondary bile acids have been observed after RYGB (Ahmad et al., 2013; Glicksman et al., 2010; Kohli et al., 2013; Patti et al., 2009) and have been linked to increased GLP-1 and reduced glucose and triglyceride levels (Nakatani et al., 2009; Patti et al., 2009; Pournaras et al., 2012; Simonen et al., 2012). The postprandial bile acid response is blunted in obesity and enhanced after RYGB, indicating that this response might be important for inducing satiety, reduced food intake, and lower body weight (Ahmad et al., 2013; Glicksman et al., 2010).

Because the composition of the bile acid pool is regulated by the gut microbiota (Sayin et al., 2013), we examined the relationship between the altered gut microbiota and bile acid pool composition after bariatric surgery. We quantified putative microbial genes for bile acid metabolism and showed that levels of *bsh* genes (for bile salt hydrolases) did not differ, while *baiB*, *baiCD*, *baiE*, *baiF*, and *baiG* (genes for the 7α-dehydroxylation of primary bile acids) increased in RYGB compared to OBS, although not significantly (Figure S3A). Fasting bile acid concentrations did not differ between RYGB, VBG, and OBS patients, but we confirmed a blunted postprandial bile acid response for OBS women and observed a slight increase in postprandial bile acid levels for VBG patients (Figures 3A and 3B), which was significant only for the secondary bile acid
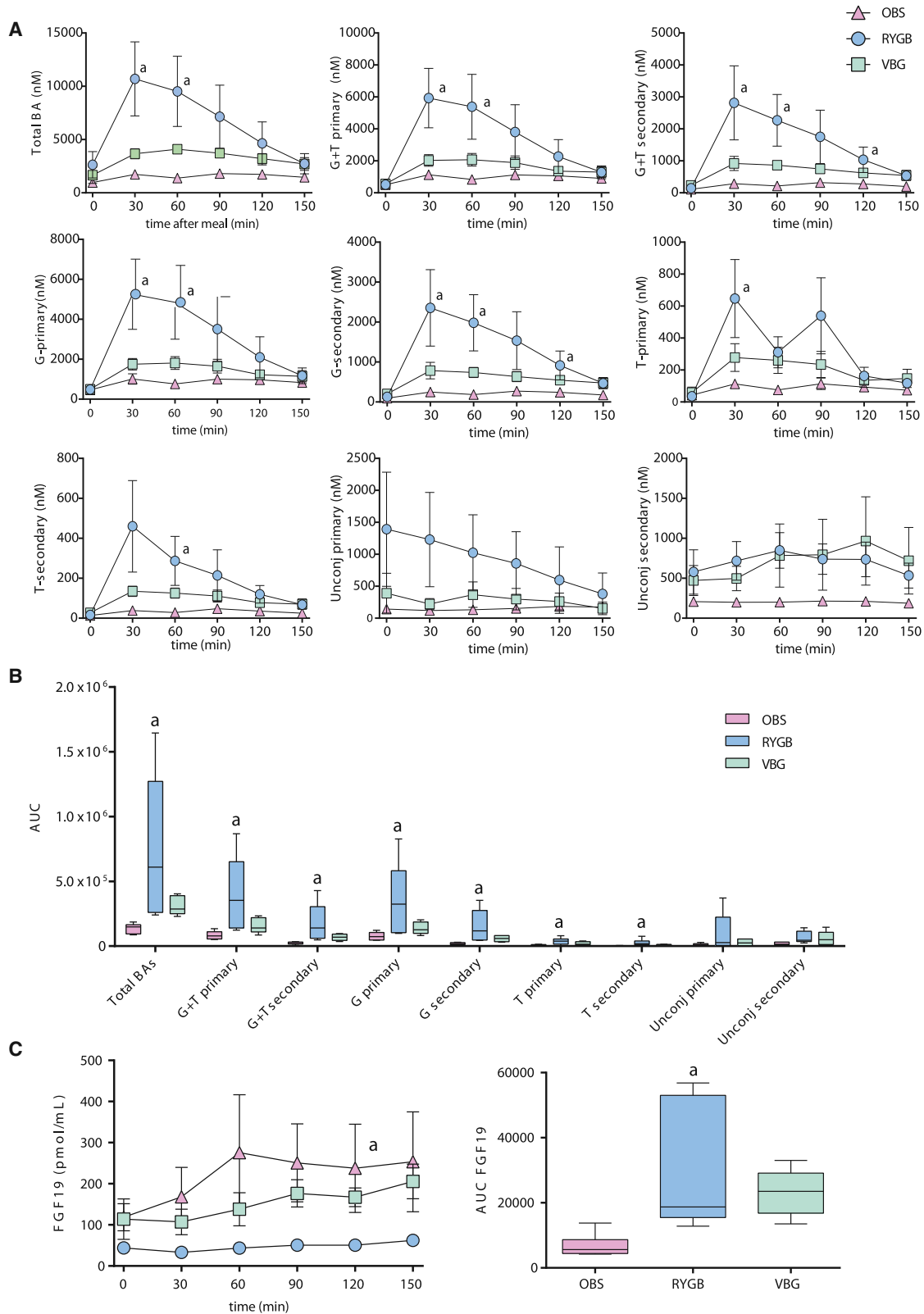
Figure 3. Postprandial Bile Acid and FGF19 Responses in RYGB, VBG, and OBS Women

(A) Circulating concentrations of total bile acids (Total BA), total conjugated primary (G+T primary), total conjugated secondary (G+T secondary), glycine-conjugated primary (G-primary), glycine-conjugated secondary (G-secondary), taurine-conjugated primary (T-primary), taurine-conjugated secondary (T-secondary), unconjugated primary, and unconjugated secondary bile acids.

(legend continued on next page)

glycine-conjugated lithocholic acid (Figure S3B). However, we observed a pronounced postprandial bile acid response in RYGB compared to OBS patients, with a significant increase in total and glycine- and taurine-conjugated bile acids, but not unconjugated bile acids (Figures 3A and 3B). The increased bile acid levels in RYGB women were attributable to increases in both primary and secondary conjugated bile acids (Figure S3B, ANOVA p < 0.05). Finally, we measured the circulating levels of FGF19, an intestinal factor that regulates bile acid, carbohydrate, lipid, and energy metabolism through bile acid-mediated activation of FXR (Beenken and Mohammadi, 2009). We observed an increased FGF19 response in RYGB women compared to OBS (Figure 3C), indicating increased FXR signaling.

Our results provide evidence for an increased abundance in RYGB microbiomes of microbial genes involved in the dehydroxylation of primary to secondary bile acids, which is in line with the increased response of secondary bile acids in RYGB patients. However, these results need to be further validated in larger cohorts and at shorter time points after bariatric surgery.

Analysis of BMI as a Possible Confounding Factor

To control for differences in BMI, we compared the gut microbiome of RYGB and VBG patients with that of non-operated women (Ob, n = 9) with BMI matched to the post-surgical BMI of the RYGB and VBG patients (BMI = 31.9 ± 2.7 [SD]) (Table S1 and S5). The Ob group was selected from a larger cohort recently analyzed with methods comparable to those used here (Karlsson et al., 2013). We found again an expansion in Proteobacteria and a reduction in several clostridial species after RYGB, and also a significant increase in the relative abundance of three *E. coli* species in VBG (Figure 4A; Table S5).

We observed differences in the genetic content of RYGB, VBG, and Ob microbiomes (Figure 4B; Table S5). Several pathways (e.g., two-component systems, fluorobenzoate degradation, and glyoxylate and dicarboxylate metabolism) and KOs (e.g., *nifA*, *pgtCAP*, *ato*, and *deg* genes) enriched in RYGB or VBG compared to OBS were also enriched in comparison to Ob microbiomes (Table S5). In particular, *torA* (K07811) was enriched in RYGB and VBG compared to both OBS and Ob (Figure S4).

These results indicate that the differences in gut microbiota composition and genetic content result from bariatric surgery and not BMI per se, since the OBS and Ob microbiomes were similar (Figure 4; Table S5). Indeed, previous studies of the gut microbiota during dietary interventions for weight loss have not reported an increase in Proteobacteria but a shift in taxa such as Bacteroidetes (Ley et al., 2006), *Eubacterium/Roseburia* (Duncan et al., 2008), and *Eubacterium rectale* (Cotillard et al., 2013). Together with these observations, our results suggest that bariatric surgery produces a specific shift in the microbiota that persists for up to a decade after surgery and is different from shifts related to dietary interventions for weight loss.

Transmission of the Human Adiposity Phenotype by Transplantation of the Gut Microbiota

To investigate whether the altered gut microbiota of bariatric surgery patients directly affects adiposity and metabolism, we transplanted the fecal microbiota of RYGB, VBG, and OBS patients into female GF mice. We observed that mice colonized with RYGB and VBG microbiota for 2 weeks accumulated 43% and 26% less body fat, respectively, than mice colonized with OBS microbiota (Figure 5A), while mice colonized with RYGB microbiota had the highest average increase in lean mass (Figures S5A–S5C); body weight gain and food intake did not differ between the groups during the 2-week colonization period (Figures S5D and S5E). In addition, we measured oxygen (O_2) consumption and carbon dioxide (CO_2) production in the mice colonized with RYGB, VGB, and OBS microbiota. Although O_2 consumption, body weight gain, and food intake did not differ during the measurements (Figures S5F–S5I), GF mice colonized with RYGB microbiota had a lower respiratory quotient ([RQ]; ratio between CO_2 produced and O_2 consumed) than mice colonized with OBS microbiota (active phase, Night1, Figure 5B) or with VBG microbiota (resting phase, Figure 5C), thus indicating decreased utilization of carbohydrates and increased utilization of lipids as fuel in recipients of RYGB microbiota.

The reduced fat mass gain in GF mice transplanted with RYGB and VBG microbiota is in agreement with our results on the composition of the gut microbiome and with a short-term human study showing an inverse correlation between *E. coli* abundance and fat mass after RYGB (Furet et al., 2010). These results are also consistent with a mouse study showing a reduced ability of the RYGB microbiota to promote adiposity (Liou et al., 2013). As we observed decreased SCFAs in RYGB and VBG samples, reduced energy harvest from the diet might be a mechanism for the reduced fat mass gain in the mice transplanted with bariatric surgery microbiota.

We also observed that mice receiving RYGB microbiota gained the least fat mass and had a reduced RQ, suggesting reduced utilization of carbohydrates and increased utilization of fat for metabolic processes. Reduced RQ has been observed in humans after RYGB and associated to reduced glucose oxidation, increased lipid oxidation, and increased plasma levels of conjugated bile acids (Simonen et al., 2012). As we found increased levels of secondary bile acids in the plasma of RYGB patients, microbial regulation of bile acid metabolism could contribute to the improved metabolic phenotype of RYGB patients by promoting increased utilization of fat, and to the superior long-term weight loss and metabolic improvements observed after RYGB compared to VBG (Sjöström et al., 2007; Werling et al., 2013a). However, as we compared the microbiomes of RYGB and VBG patients matched for weight loss, future studies of the microbiome from patients achieving different levels of weight and fat loss are required to validate our findings.

(B) Tukey box plots showing the area under the curve (AUC) as a measure of the bile acid postprandial responses.
(C) Circulating concentrations of FGF19 and AUC showing FGF19 postprandial response in RYGB, VBG, and OBS women.
Plasma samples were collected during fasting and every 30 min for 2.5 hr after a standard meal. Samples from colecystectomized patients (one in the RYGB and one in the VBG group) were excluded from the analysis, and plasma from one VBG woman could not be obtained, so the results represent the mean ± SEM for six RYGB, five VBG, and seven OBS women. [a] p < 0.05 according to one-way ANOVA with Tukey's correction for multiple comparisons for RYGB compared to OBS. See also Figure S3.
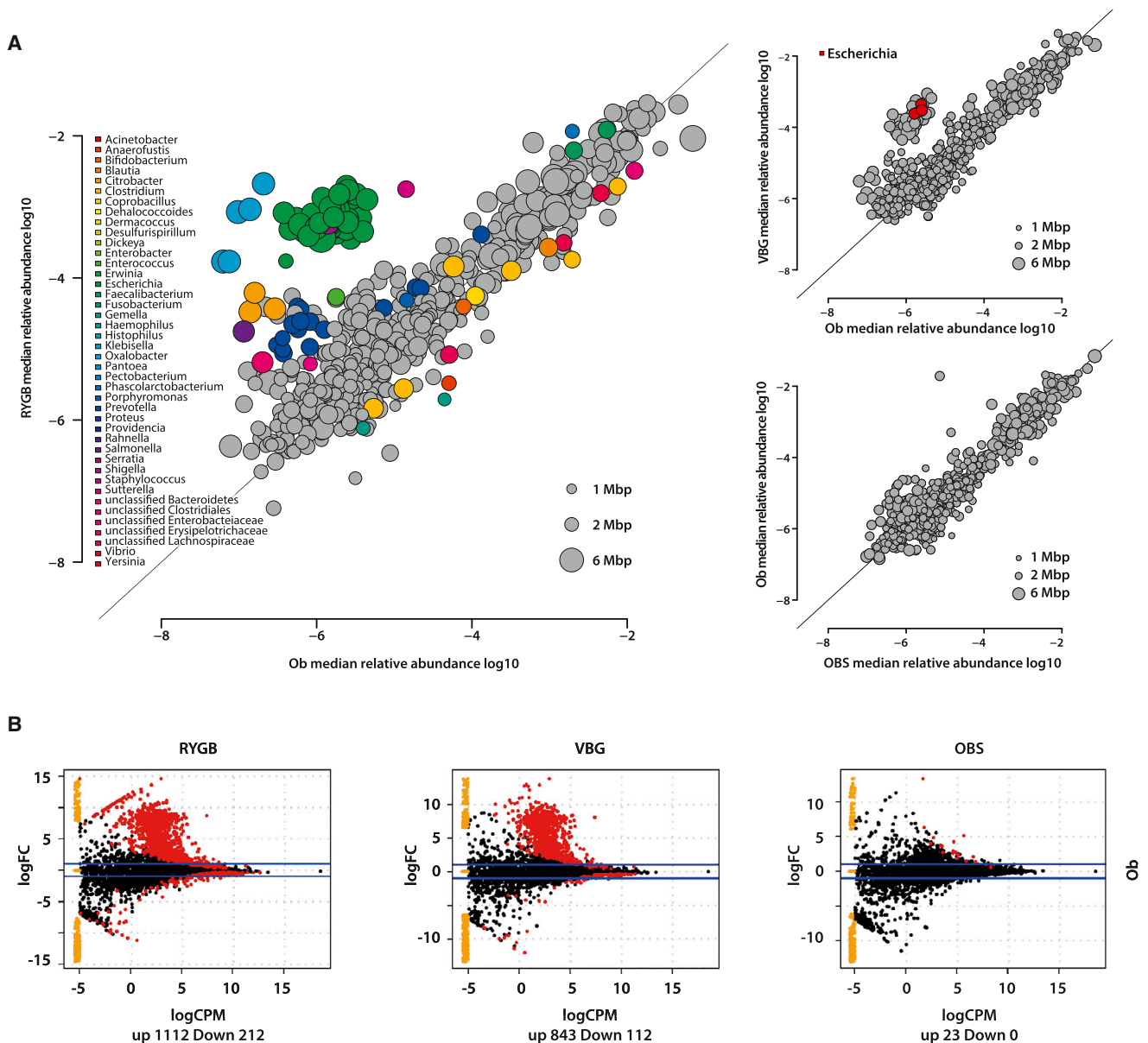
Figure 4. Gut Microbiome of RYGB and VBG Women in Comparison to Non-Operated Women (Ob) with BMI Matched to the Post-Surgical BMI of the Bariatric Surgery Patients

(A) Gut microbiota composition. Scatter plot of median species abundance in RYGB and Ob, in VBG and Ob, and in Ob and OBS women. The genus affiliations of differentially abundant species are indicated by color (Adj. p < 0.05, Wilcoxon rank-sum test).

(B) Functional differences in the microbiomes measured by the abundance of KOs. Each spot represents a KO, and red spots represent KOs whose abundance is significantly different. The number of KOs significantly increased (up) and depleted (down) is shown under each plot. The direction of change is defined as up being the title above and down being the title to the right of each plot. FC, fold change; CPM, counts per million. See also Table S5 and Figure S4.

PERSPECTIVE

Our study shows that bariatric surgery has long-term effects on the composition and functional capacity of the gut microbiota and that these changes have the potential to modulate host metabolic regulation, thus adding evidence for the transmissibility of the human adiposity phenotype through the gut microbiota.

Our results also show that two different bariatric surgery procedures, namely RYGB and VBG, have similar long-term effects on the gut microbiome in women matched for BMI and fat mass loss. However, the two bariatric surgery procedures might result in different functionality due to different intestinal environmental conditions, as we exemplified for TMA/TMAO metabolism. Importantly, the changes in the microbiome were not dependent on BMI or degree of weight and fat mass loss,
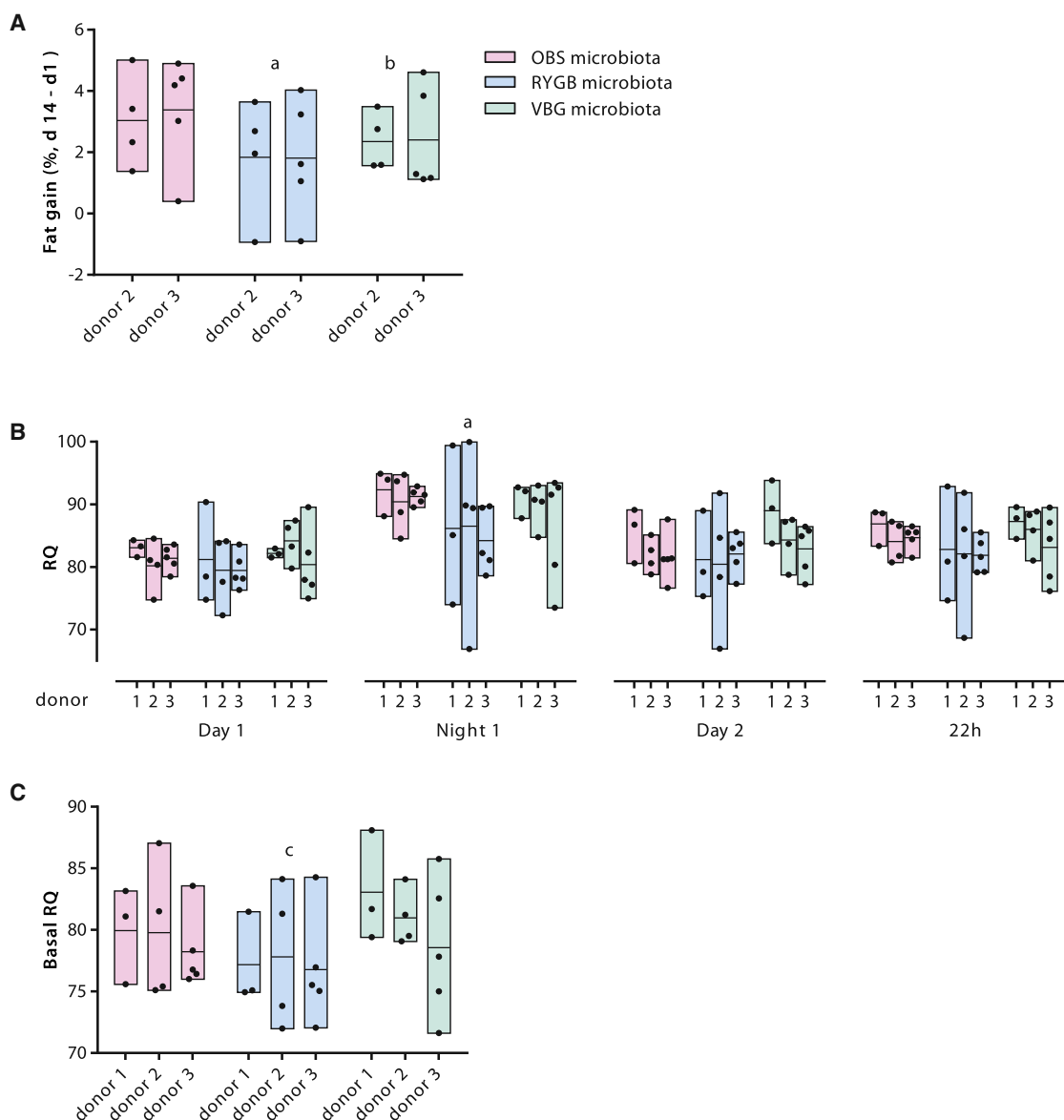
Figure 5. The Gut Microbiota Influences Fat Accumulation and Metabolism in Colonized Mice

(A) Fat gain in mice colonized with human stools from OBS, RYGB, and VBG women. Fat gain was calculated as the difference between fat content normalized over body weight at the end of the experiment (d14) and fat content normalized over body weight 1 day after colonization (d1). The results presented were obtained from colonization of GF mice with fecal microbiota from two patients in each of the RYGB, VBG, and OBS groups (four to five mice per donor microbiota).

(B) RQ (ratio between CO_2 produced and O_2 consumed) calculated for the light and dark phases and for the overall 22 hr period in the Somedic chamber.

(C) RQ in the resting phase (basal RQ, calculated as the average RQ for the lowest 10 min average of O_2 consumption).

The results presented in (B) and (C) were obtained from colonization of GF mice with fecal microbiota from three patients in each of the RYGB, VBG, and OBS groups (3–5 mice per donor microbiota).

Bars show the results of colonization with the same donor microbiota, with black dots showing individual mice and lines indicating the mean. Statistical significance of differences between the means was tested by one-way ANOVA with Tukey's correction for multiple comparisons ([a] $p < 0.05$ for RYGB compared to OBS, [b] $p < 0.05$ for VBG compared to OBS, and [c] $p < 0.05$ for RYGB compared to VBG). See also Figure S5.

thus revealing shifts in the gut microbiota that were specific to bariatric surgery.

EXPERIMENTAL PROCEDURES

Subjects and Sample Collection

The operated women included in this study participated in a previous clinical trial for the measurement of energy expenditure after RYGB (n = 7) and VBG (n = 7) (Werling et al., 2013b). The clinical trial and the enrollment of subjects were described previously (Werling et al., 2013b). We also included samples from severely obese women with a BMI similar to the mean pre-surgical BMI of the operated women (OBS, n = 7), and these women underwent measurements of energy expenditure as the RYGB and VBG patients. None of the women included in our study had diabetes. However, the RYGB patients had significantly reduced fasting insulin compared with OBS, whereas there was a trend toward reduction in the VBG patients (Table S1).

Blood samples were collected during the measurements of energy expenditure in the indirect calorimetry chamber; 17 out of 21 stool samples were also collected during the measurements, while the remaining four samples were collected at home 2 to 8 days after. Stool samples collected in the calorimetry chamber were immediately frozen at $-80°C$. Samples collected at home were kept at room temperature and mailed to the hospital, where they arrived within 24 hr from collection and were immediately frozen at $-80°C$. The 21 women in our study did no use antibiotics for at least 6 weeks before inclusion in the study. The studies were performed in accordance with the Declaration of Helsinki and were approved by the Regional Ethical Review Board in Gothenburg, Sweden (no: 359-09 and 740-10). All study participants were informed verbally and in writing and signed a consent form.

Quantification of Organic Acids, TMAO, and Bile Acids

Fecal SCFAs and BCFAs were determined by gas chromatography-mass spectrometry (GC-MS) as previously described (Ryan et al., 2014). TMAO, choline, betaine, and bile acids were extracted from plasma samples and measured by ultra-performance liquid chromatography-tandem mass spectrometry (UPLC-MS/MS). Detailed methods are provided in the Supplemental Experimental Procedures.

DNA Extraction and Metagenome Data Analysis

Genomic DNA was extracted from fecal samples using repeated bead beating (Salonen et al., 2010). DNA fragments of approximately 300 bp were sequenced on an Illumina HiSeq 2000 instrument. Metagenomic sequence data was analyzed using methods from the MEDUSA platform (Karlsson et al., 2012, 2014). The statistical analysis was performed in the software R (R Core Team, 2012). All p values were corrected for multiple testing with the method from Benjamini and Hochberg (1995). Detailed methods are provided in the Supplemental Experimental Procedures.

Mouse Experiments

For microbiota transplantations, we selected stool samples from three RYGB, three VBG, and three OBS patients who did not use medications and did not receive cholecystectomy and used these samples to colonize GF Swiss Webster female mice in three independent experiments. Mice were colonized by oral gavage of fecal slurry at 8–10 weeks of age, for a period of 2 weeks; more details are provided in the Supplemental Experimental Procedures. Mice were fed autoclaved chow and sterile water; food consumption and body weight were recorded 1, 7, and 14 days after colonization. In two of the experiments, body composition was determined with an EchoMRI instrument (EchoMRI) 1 and 14 days after colonization. All mice were analyzed by indirect calorimetry in the Somedic INCA system (Somedic, Hörby) for measurements of O_2 consumption and CO_2 production. All animal experiments were approved by the Gothenburg Animal Ethics Committee.

ACCESSION NUMBERS

Metagenomic sequence data has been deposited at the European Nucleotide Archive under the accession number ENA: ERP009310.

SUPPLEMENTAL INFORMATION

Supplemental Information includes five figures, five tables, and Supplemental Experimental Procedures and can be found with this article online at http://dx.doi.org/10.1016/j.cmet.2015.07.009.

AUTHOR CONTRIBUTIONS

M.W., T.O., L.F., C.W.I.R., and F.B. conceived and designed the human study. V.T. and F.B. designed and analyzed microbiota transplantation experiments in GF mice. M.S. developed the methods and quantified the levels of TMAO, choline, betaine, and bile acids. P.K.-D. quantified the levels of SCFAs and BCFAs. V.T., F.K., and M.W. performed the experiments. F.K. and J.N. analyzed the gut microbiota sequence data. V.T., F.K., and F.B. wrote the manuscript. All authors were involved in the discussion of the results and commented on the manuscript.

CONFLICTS OF INTEREST

ACKNOWLEDGMENTS

REFERENCES

Ahmad, N.N., Pfalzer, A., and Kaplan, L.M. (2013). Roux-en-Y gastric bypass normalizes the blunted postprandial bile acid excursion associated with obesity. Int. J. Obes. 37, 1553–1559.

Amar, J., Chabo, C., Waget, A., Klopp, P., Vachoux, C., Bermúdez-Humarán, L.G., Smirnova, N., Bergé, M., Sulpice, T., Lahtinen, S., et al. (2011). Intestinal mucosal adherence and translocation of commensal bacteria at the early onset of type 2 diabetes: molecular mechanisms and probiotic treatment. EMBO Mol. Med. 3, 559–572.

Barrett, E.L., and Kwan, H.S. (1985). Bacterial reduction of trimethylamine oxide. Annu. Rev. Microbiol. 39, 131–149.

Beenken, A., and Mohammadi, M. (2009). The FGF family: biology, pathophysiology and therapy. Nat. Rev. Drug Discov. 8, 235–253.

Benjamini, Y., and Hochberg, Y. (1995). Controlling the False Discovery Rate - a Practical and Powerful Approach to Multiple Testing. J. Roy. Stat. Soc. B. Met. 57, 289–300.

Cani, P.D., Amar, J., Iglesias, M.A., Poggi, M., Knauf, C., Bastelica, D., Neyrinck, A.M., Fava, F., Tuohy, K.M., Chabo, C., et al. (2007). Metabolic endotoxemia initiates obesity and insulin resistance. Diabetes 56, 1761–1772.

Cotillard, A., Kennedy, S.P., Kong, L.C., Prifti, E., Pons, N., Le Chatelier, E., Almeida, M., Quinquis, B., Levenez, F., Galleron, N., et al.; ANR MicroObes consortium (2013). Dietary intervention impact on gut microbial gene richness. Nature 500, 585–588.

Duncan, S.H., Lobley, G.E., Holtrop, G., Ince, J., Johnstone, A.M., Louis, P., and Flint, H.J. (2008). Human colonic microbiota associated with diet, obesity and weight loss. Int. J. Obes. 32, 1720–1724.

Duncan, S.H., Louis, P., Thomson, J.M., and Flint, H.J. (2009). The role of pH in determining the species composition of the human colonic microbiota. Environ. Microbiol. 11, 2112–2122.

Flint, H.J., Scott, K.P., Louis, P., and Duncan, S.H. (2012). The role of the gut microbiota in nutrition and health. Nat. Rev. Gastroenterol. Hepatol. 9, 577–589.

Furet, J.P., Kong, L.C., Tap, J., Poitou, C., Basdevant, A., Bouillot, J.L., Mariat, D., Corthier, G., Doré, J., Henegar, C., et al. (2010). Differential adaptation of human gut microbiota to bariatric surgery-induced weight loss: links with metabolic and low-grade inflammation markers. Diabetes 59, 3049–3057.

Glicksman, C., Pournaras, D.J., Wright, M., Roberts, R., Mahon, D., Welbourn, R., Sherwood, R., Alaghband-Zadeh, J., and le Roux, C.W. (2010). Postprandial plasma bile acid responses in normal weight and obese subjects. Ann. Clin. Biochem. 47, 482–484.

Graessler, J., Qin, Y., Zhong, H., Zhang, J., Licinio, J., Wong, M.L., Xu, A., Chavakis, T., Bornstein, A.B., Ehrhart-Bornstein, M., et al. (2013). Metagenomic sequencing of the human gut microbiome before and after bariatric surgery in obese patients with type 2 diabetes: correlation with inflammatory and metabolic parameters. Pharmacogenomics J. 13, 514–522.

Hylemon, P.B., Zhou, H., Pandak, W.M., Ren, S., Gil, G., and Dent, P. (2009). Bile acids as regulatory molecules. J. Lipid Res. 50, 1509–1520.

Karlsson, F.H., Fåk, F., Nookaew, I., Tremaroli, V., Fagerberg, B., Petranovic, D., Bäckhed, F., and Nielsen, J. (2012). Symptomatic atherosclerosis is associated with an altered gut metagenome. Nat. Commun. 3, 1245.

Karlsson, F.H., Tremaroli, V., Nookaew, I., Bergström, G., Behre, C.J., Fagerberg, B., Nielsen, J., and Bäckhed, F. (2013). Gut metagenome in European women with normal, impaired and diabetic glucose control. Nature 498, 99–103.

Karlsson, F.H., Nookaew, I., and Nielsen, J. (2014). Metagenomic data utilization and analysis (MEDUSA) and construction of a global gut microbial gene catalogue. PLoS Comput. Biol. 10, e1003706.

Kohli, R., Bradley, D., Setchell, K.D., Eagon, J.C., Abumrad, N., and Klein, S. (2013). Weight loss induced by Roux-en-Y gastric bypass but not laparoscopic adjustable gastric banding increases circulating bile acids. J. Clin. Endocrinol. Metab. 98, E708–E712.

Kong, L.C., Tap, J., Aron-Wisnewsky, J., Pelloux, V., Basdevant, A., Bouillot, J.L., Zucker, J.D., Doré, J., and Clément, K. (2013). Gut microbiota after gastric bypass in human obesity: increased richness and associations of bacterial genera with adipose tissue genes. Am. J. Clin. Nutr. 98, 16–24.

Le Chatelier, E., Nielsen, T., Qin, J., Prifti, E., Hildebrand, F., Falony, G., Almeida, M., Arumugam, M., Batto, J.M., Kennedy, S., et al.; MetaHIT consortium (2013). Richness of human gut microbiome correlates with metabolic markers. Nature 500, 541–546.

le Roux, C.W., and Bloom, S.R. (2005). Why do patients lose weight after Roux-en-Y gastric bypass? J. Clin. Endocrinol. Metab. 90, 591–592.

Lefebvre, P., Cariou, B., Lien, F., Kuipers, F., and Staels, B. (2009). Role of bile acids and bile acid receptors in metabolic regulation. Physiol. Rev. 89, 147–191.

Ley, R.E., Bäckhed, F., Turnbaugh, P., Lozupone, C.A., Knight, R.D., and Gordon, J.I. (2005). Obesity alters gut microbial ecology. Proc. Natl. Acad. Sci. USA 102, 11070–11075.

Ley, R.E., Turnbaugh, P.J., Klein, S., and Gordon, J.I. (2006). Microbial ecology: human gut microbes associated with obesity. Nature 444, 1022–1023.

Liou, A.P., Paziuk, M., Luevano, J.M., Jr., Machineni, S., Turnbaugh, P.J., and Kaplan, L.M. (2013). Conserved shifts in the gut microbiota due to gastric bypass reduce host weight and adiposity. Sci. Transl. Med. 5, 178ra41.

Mascher, T., Helmann, J.D., and Unden, G. (2006). Stimulus perception in bacterial signal-transducing histidine kinases. Microbiol. Mol. Biol. Rev. 70, 910–938.

Miras, A.D., and le Roux, C.W. (2013). Mechanisms underlying weight loss after bariatric surgery. Nat. Rev. Gastroenterol. Hepatol. 10, 575–584.

Mukhopadhya, I., Hansen, R., El-Omar, E.M., and Hold, G.L. (2012). IBD-what role do Proteobacteria play? Nat. Rev. Gastroenterol. Hepatol. 9, 219–230.

Nakatani, H., Kasama, K., Oshiro, T., Watanabe, M., Hirose, H., and Itoh, H. (2009). Serum bile acid along with plasma incretins and serum high-molecular weight adiponectin levels are increased after bariatric surgery. Metabolism 58, 1400–1407.

Olbers, T., Björkman, S., Lindroos, A., Maleckas, A., Lönn, L., Sjöström, L., and Lönroth, H. (2006). Body composition, dietary intake, and energy expenditure after laparoscopic Roux-en-Y gastric bypass and laparoscopic vertical banded gastroplasty: a randomized clinical trial. Ann. Surg. 244, 715–722.

Oliveira, A.P., Patil, K.R., and Nielsen, J. (2008). Architecture of transcriptional regulatory circuits is knitted over the topology of bio-molecular interaction networks. BMC Syst. Biol. 2, 17.

Patil, K.R., and Nielsen, J. (2005). Uncovering transcriptional regulation of metabolism by using metabolic network topology. Proc. Natl. Acad. Sci. USA 102, 2685–2689.

Patti, M.E., Houten, S.M., Bianco, A.C., Bernier, R., Larsen, P.R., Holst, J.J., Badman, M.K., Maratos-Flier, E., Mun, E.C., Pihlajamaki, J., et al. (2009). Serum bile acids are higher in humans with prior gastric bypass: potential contribution to improved glucose and lipid metabolism. Obesity (Silver Spring) 17, 1671–1677.

Pournaras, D.J., Glicksman, C., Vincent, R.P., Kuganolipava, S., Alaghband-Zadeh, J., Mahon, D., Bekker, J.H., Ghatei, M.A., Bloom, S.R., Walters, J.R., et al. (2012). The role of bile after Roux-en-Y gastric bypass in promoting weight loss and improving glycaemic control. Endocrinology 153, 3613–3619.

Qin, J., Li, R., Raes, J., Arumugam, M., Burgdorf, K.S., Manichanh, C., Nielsen, T., Pons, N., Levenez, F., Yamada, T., et al.; MetaHIT Consortium (2010). A human gut microbial gene catalogue established by metagenomic sequencing. Nature 464, 59–65.

Qin, J., Li, Y., Cai, Z., Li, S., Zhu, J., Zhang, F., Liang, S., Zhang, W., Guan, Y., Shen, D., et al. (2012). A metagenome-wide association study of gut microbiota in type 2 diabetes. Nature 490, 55–60.

R Core Team (2012). R: A Language and Environment for Statistical Computing (Vienna).

Ryan, K.K., Tremaroli, V., Clemmensen, C., Kovatcheva-Datchary, P., Myronovych, A., Karns, R., Wilson-Pérez, H.E., Sandoval, D.A., Kohli, R., Bäckhed, F., and Seeley, R.J. (2014). FXR is a molecular target for the effects of vertical sleeve gastrectomy. Nature 509, 183–188.

Salonen, A., Nikkilä, J., Jalanka-Tuovinen, J., Immonen, O., Rajilić-Stojanović, M., Kekkonen, R.A., Palva, A., and de Vos, W.M. (2010). Comparative analysis of fecal DNA extraction methods with phylogenetic microarray: effective recovery of bacterial and archaeal DNA using mechanical cell lysis. J. Microbiol. Methods 81, 127–134.

Sayin, S.I., Wahlström, A., Felin, J., Jäntti, S., Marschall, H.U., Bamberg, K., Angelin, B., Hyötyläinen, T., Orešič, M., and Bäckhed, F. (2013). Gut microbiota regulates bile acid metabolism by reducing the levels of tauro-beta-muricholic acid, a naturally occurring FXR antagonist. Cell Metab. 17, 225–235.

Simonen, M., Dali-Youcef, N., Kaminska, D., Venesmaa, S., Käkelä, P., Pääkkönen, M., Hallikainen, M., Kolehmainen, M., Uusitupa, M., Moilanen, L., et al. (2012). Conjugated bile acids associate with altered rates of glucose and lipid oxidation after Roux-en-Y gastric bypass. Obes. Surg. 22, 1473–1480.

Sjöström, L., Narbro, K., Sjöström, C.D., Karason, K., Larsson, B., Wedel, H., Lystig, T., Sullivan, M., Bouchard, C., Carlsson, B., et al.; Swedish Obese Subjects Study (2007). Effects of bariatric surgery on mortality in Swedish obese subjects. N. Engl. J. Med. 357, 741–752.

Sjöström, L., Peltonen, M., Jacobson, P., Sjöström, C.D., Karason, K., Wedel, H., Ahlin, S., Anveden, Å., Bengtsson, C., Bergmark, G., et al. (2012). Bariatric surgery and long-term cardiovascular events. JAMA 307, 56–65.

Smith, M.I., Yatsunenko, T., Manary, M.J., Trehan, I., Mkakosya, R., Cheng, J., Kau, A.L., Rich, S.S., Concannon, P., Mychaleckyj, J.C., et al. (2013). Gut microbiomes of Malawian twin pairs discordant for kwashiorkor. Science 339, 548–554.

Tang, W.H., Wang, Z., Levison, B.S., Koeth, R.A., Britt, E.B., Fu, X., Wu, Y., and Hazen, S.L. (2013). Intestinal microbial metabolism of phosphatidylcholine and cardiovascular risk. N. Engl. J. Med. 368, 1575–1584.

Tremaroli, V., and Bäckhed, F. (2012). Functional interactions between the gut microbiota and host metabolism. Nature 489, 242–249.

Turnbaugh, P.J., Ley, R.E., Mahowald, M.A., Magrini, V., Mardis, E.R., and Gordon, J.I. (2006). An obesity-associated gut microbiome with increased capacity for energy harvest. Nature 444, 1027–1031.

Turnbaugh, P.J., Hamady, M., Yatsunenko, T., Cantarel, B.L., Duncan, A., Ley, R.E., Sogin, M.L., Jones, W.J., Roe, B.A., Affourtit, J.P., et al. (2009). A core gut microbiome in obese and lean twins. Nature 457, 480–484.

Wang, Z., Klipfell, E., Bennett, B.J., Koeth, R., Levison, B.S., Dugar, B., Feldstein, A.E., Britt, E.B., Fu, X., Chung, Y.-M., et al. (2011). Gut flora metabolism of phosphatidylcholine promotes cardiovascular disease. Nature *472*, 57–63.

Werling, M., Fändriks, L., Björklund, P., Maleckas, A., Brandberg, J., Lönroth, H., le Roux, C.W., and Olbers, T. (2013a). Long-term results of a randomized clinical trial comparing Roux-en-Y gastric bypass with vertical banded gastroplasty. Br. J. Surg. *100*, 222–230.

Werling, M., Olbers, T., Fändriks, L., Bueter, M., Lönroth, H., Stenlöf, K., and le Roux, C.W. (2013b). Increased postprandial energy expenditure may explain superior long term weight loss after Roux-en-Y gastric bypass compared to vertical banded gastroplasty. PLoS ONE *8*, e60280.

Zhang, H., DiBaise, J.K., Zuccolo, A., Kudrna, D., Braidotti, M., Yu, Y., Parameswaran, P., Crowell, M.D., Wing, R., Rittmann, B.E., and Krajmalnik-Brown, R. (2009). Human gut microbiota in obesity and after gastric bypass. Proc. Natl. Acad. Sci. USA *106*, 2365–2370.

Supplemental Information

Roux-en-Y Gastric Bypass and Vertical Banded

Gastroplasty Induce Long-Term Changes on the Human

Gut Microbiome Contributing to Fat Mass Regulation

Valentina Tremaroli, Fredrik Karlsson, Malin Werling, Marcus Ståhlman, Petia Kovatcheva-Datchary, Torsten Olbers, Lars Fändriks, Carel W. le Roux, Jens Nielsen, and Fredrik Bäckhed

Supplemental Experimental Procedures

Metagenomic Data Quality Control

Sequence reads were trimmed from the 3' end with Fastx quality trimmer using quality threshold of 20. Read pairs with either read shorter than 35 bp were removed. Read pairs aligning to the human genome (NCBI version 37) were removed using bowtie with settings "-n 2 -l 35 -e 200 --best -p 8 --chunkmbs 1024 -X 600 –tryhard". The set of high-quality reads was used in further analysis.

Alignment to Reference Genomes and Taxonomical Analysis

A reference catalogue of 2382 reference genomes from the NCBI and HMP databases was collected (Table S2). The reference genomes were split into two Bowtie indexes. High-quality reads were aligned to each index using Bowtie (Langmead et al., 2009) with the following parameters: -n 2 -l 35 -e 300 --best -p 8 --chunkmbs 1024 -X 600 –tryhard. The results from the two indexes were merged by selecting the alignment with fewest mismatches and more than 90% identities; if a read was aligned to a reference genome with the same number of mismatches, each genome was assigned 1/2 read. The relative abundance of each genome was calculated by summing the number of reads aligned to that genome divided by the total number of reads and scaled by the genome size. In each subject, the relative abundance was scaled to sum to one. Taxonomic information for each genome was downloaded from the NCBI taxonomy database. By summing the relative abundance of child ranks, the relative abundance of taxonomic parent ranks was calculated.

Alignment to Reference Gene Catalogue

The human gut microbial gene catalogue generated by MetaHIT (Qin et al., 2010) was downloaded and indexed with Bowtie2 (Langmead and Salzberg, 2012). The metagenomic sequence reads were aligned with Bowtie2 using the default parameters and aligning reads with at least 90% sequence identity were counted. The provided annotation of the genes to KEGG was used and the aligning reads to each KO was summed.

Statistical Analysis

The statistical analysis was performed in the software R (R Core Team, 2012). The relative abundance of species and genera between groups was tested with Wilcoxon rank-sum test. P values were corrected for multiple testing with the method from Benjamini and Hochberg (Benjamini and Hochberg, 1995). Species with a relative abundance above 10^{-5} in any subject were included in the analysis.

For the functional analysis, the R package edgeR was used, which uses the read counts to assess the differential abundance of KOs between groups. The read counts for each KO were loaded into R and the dispersion was calculated with the functions estimateGLMCommonDisp(), estimateGLMTrendedDisp() and estimateGLMTagwiseDisp(). For further analysis, the tagwise dispersion was used in the glmFit() function. The individual comparisons between groups were

performed with the glmLRT() function by pairwise comparing the groups. P values were adjusted with the method from Benjamini and Hochberg (Benjamini and Hochberg, 1995). In the analysis using edgeR, if not stated otherwise, default parameters were used.

To analyze the results from the abundance of KOs in the context of pathways, the KO differential adjusted P values and direction of change were analyzed together with the KO pathway membership using the Reporter Feature algorithm as implemented in the R package Piano (Varemo et al., 2013). The null distribution was used as significance method.

Bile salt hydrolases annotated to the K01442 in the MetaHIT gene catalogue were extracted and annotated to the two types of bile salt hydrolases, Bsh1 and Bsh2, described by Fang et al. (Fang et al., 2009). Sequences for *bsh1* and *bsh2* genes were downloaded from NCBI Genebank with accessions 221062093, 221062123, 221062125, 221062129, 221062139 as representatives for bsh1 and 221062141, 221062143 as representatives for bsh2. MetaHIT genes with annotation to K01442 were aligned to the catalogue of *bsh* genes and the best hits with an E-value score below 10-5 were annotated as either *bsh1* or *bsh2*, for a total of 469 sequences. The pathway for 7α-dehydroxylation of bile acids is responsible for the dehydroxylation of primary bile acids and formation of secondary bile acids by the gut microbiota, and is encoded by the polycistronic bile acid-inducible (*bai*) operon, which contains genes for 8 enzymes (*baiA*, *baiB*, *baiCD*, *baiE*, *baiF*, *baiG*, *baiH* and *baiI*) (Ridlon et al., 2006). This pathway is not completely reconstructed in KEGG and therefore the genes in the MetaHIT gene catalogue were functionally annotated to enzymes in this pathway. 16 protein sequences from two organisms known to carry this pathway, Clostridium hylemonae DSM 15053 (Ridlon et al., 2010) and Clostridium scindens VPI 12708 (Kitahara et al., 2000) were downloaded from the ENA database at EMBL-EBI (http://www.ebi.ac.uk/ena/). The MetaHIT genes were aligned to the 7α-dehydroxylation sequences using UBLAST (Edgar, 2010) with an E-value cutoff of 10^{-5}. The candidates were then aligned to the full version of KEGG including the Bai proteins and only genes with a best hit to Bai proteins in this database were re-annotated. In total 70 MetaHIT genes were re-annotated to *bai* genes. *bsh* and *bai* gene abundances were tested between groups together with KEGG KOs as described above.

Measurement of SCFAs and BCFAs

GC-MS was used for measurement of organic acids in RYGB, VBG and OBS fecal samples. 70-230 mg of frozen fecal material were transferred to glass tubes (16 x 125 mm) fitted with a screw cap, and a volume of 100 µl of internal standards stock solution ([1-13C]acetate and [2H6]propionate 1 M, [13C4]butyrate 0.5 M, [1-13C1]isobutyrate and [1-13C]isovalerate 0.1 M) was added to the tubes. Prior to extraction samples were freeze-dried at -50 ℃ for 3 h (yield 25 - 75 mg dry weight). After acidification with 50 µl of 37% HCl, the organic acids were extracted twice in 2 ml of diethyl ether. A 500 µl aliquot of the extracted sample was mixed together with 50 µl of N-tert-butyldimethylsilyl-N-methyltrifluoracetamide (MTBSTFA; Sigma) at room temperature. 1 µl of the resulting derivatized material was injected into a gas chromatograph (Agilent Technologies 7890 A) coupled to a mass spectrometer detector (Agilent Technologies 5975 C). A linear temperature gradient was used: the initial temperature of 65 ℃ was held for 6

minutes, increased to 260 ℃ (15 ℃*min-1) and then to 280 ℃ for 5 minutes. The injector and transfer line temperatures were 250 ℃. Quantitation was completed in selected ion monitoring acquisition mode by comparison to labelled internal standards, and the following m/z ratios were: 117 (acetic acid), 131 (propionic acid), 145 (butyric acid), 146 (isobutyric acid), 159 (isovaleric acid), 121 ([2H2]- and [1-13C]acetate), 136 ([2H5]propionate), 146 ([1-13C1]isobutyrate), 149 ([13C4] butyrate), 160 ([1-13C]isovalerate).

Measurement of TMAO, choline and betaine

TMAO was extracted from 25 µl of plasma with 250 µl of methanol containing 250 nM of d9-TMAO (Cambridge Isotopes Laboratories, Andover, MA, USA) as internal standard. After 10 minutes of vigorous vortexing and 10 minutes of centrifugation at 20000 g, a 50 µl aliquot of the supernatant was diluted with 450 µl of acetonitrile:methanol (3:1). A 5 µl aliquot was then injected onto a UPLC-MS/MS system and TMAO was separated on a BEH HILIC column (2.1 x 100 mm with 1.7 µm particle size) (Waters, Milford, MA, USA), with mobile phases consisting of acetonitrile with 0.2% formic acid (A) and water with 10 mM ammonium acetate and 0.2% formic acid (B). The gradient started with 1 minute of isocratic elution with 15% B. B was increased to 70% over the next 5 minutes, and held at 70% for another 2 minutes. The mobile phase composition was returned to 15% B and the column was equilibrated for 3 minutes to give a total runtime of 10 minutes per sample. The flow rate was 400 µl/min. The detection was made using a QTRAP 5500 instrument (AB Sciex, Toronto Canada) running in positive multiple-reaction monitoring (MRM) mode. The transitions that were monitored were m/z 76 to m/z 58 for the endogenous TMAO and m/z 85 to m/z 66 for the internal standard. TMAO was quantified using an external standard curve with TMAO obtained from Sigma-Aldrich (Stockholm, Sweden).

Betaine and choline were extracted and diluted with the same method used to extract TMAO. A 5 µl aliquot was analyzed using the same instrumental set-up and the same BEH HILIC column as for TMAO but with mobile phases and gradient according to a previously published method (Kirsch et al., 2010). Betaine and choline were quantified using an external standard curve with betaine and choline obtained from Sigma-Aldrich (Stockholm, Sweden).

Measurement of bile acids and FGF19

The extraction and analysis of bile acids were based on a previously published method for the targeted determination of bile acids by UPLC-MS (Garcia-Canaveras et al., 2014). Bile acids were extracted from 50 µl of plasma using protein precipitation with 10 volumes of internal standard-containing methanol. After vortexing and centrifugation, the supernatant was evaporated and reconstituted in 200 µl of methanol:water (1:1). Bile acids (5µl injected) were separated using water with 7.5 mM ammonium acetate and 0.019% formic acid at a pH 4.5 as mobile phase A, and acetonitrile with 0.1% formic acid as phase B. The separation was made using gradient elution on a Kinetex C18 column (2.1x100 mm with 1.7 µm particles) (Phenomenex, Torrance, CA, USA) kept at 60 ℃. The gradient started with 1 minute of isocratic elution with 25% B, which was increased to 35% over the next 4 minutes. During the next 9.5 minutes B increased

from 35% to 95%. After one minute of isocratic elution the gradient was quickly returned to 25% B and the column was equilibrated for 2.5 min to give a total runtime of 18 minutes per sample. The flow rate was 400 µl/min. Detection was made on a QTRAP 5500 instrument (Sciex, Toronto, Canada) with MRM in negative mode. Bile acid standards were obtained from Sigma-Aldrich (Sweden, TCA, TUDCA, TCDCA, TDCA, TLCA, GCA, GCDCA, GDCA, GLCA, CA, UDCA, CDCA, DCA, LCA), CDN isotopes (Quebec, Canada, d4GCDCA, d4GLCA, d4GCA, d4GUDCA, d4CDCA, d4UDCA, d4LCA) and Toronto Research Chemicals (Downsview, Ontario, Canada, d4TCA).

Plasma FGF19 concentrations were measured by quantitative enzyme-linked immunosorbent assay with the human FGF19 Quantikine ELISA kit (R&D Systems, UK) according to the manufacturer's instructions.

Mouse Experiments

For microbiota transplantations approximately 500 mg of frozen stool samples were cut in an anaerobic Coy chamber and suspended in 5 ml of phosphate-buffered saline containing 0.2 g/l Na2S and 0.5 g/l cysteine as reducing agents. Mice were colonized by oral gavage of 200 µl of fecal slurry. Mice that received fecal microbiota from the same individual were housed in the same cage in the isocage system (Tecniplast, Italy).

Supplemental References

Benjamini, Y., and Hochberg, Y. (1995). Controlling the False Discovery Rate - a Practical and Powerful Approach to Multiple Testing. J Roy Stat Soc B Met *57*, 289-300.

Edgar, R.C. (2010). Search and clustering orders of magnitude faster than BLAST. Bioinformatics *26*, 2460-2461.

Fang, F., Li, Y., Bumann, M., Raftis, E.J., Casey, P.G., Cooney, J.C., Walsh, M.A., and O'Toole, P.W. (2009). Allelic variation of bile salt hydrolase genes in Lactobacillus salivarius does not determine bile resistance levels. Journal of bacteriology *191*, 5743-5757.

Garcia-Canaveras, J.C., Donato, M.T., and Lahoz, A. (2014). Ultra-performance liquid chromatography-mass spectrometry targeted profiling of bile acids: application to serum, liver tissue, and cultured cells of different species. Methods in molecular biology *1198*, 233-247.

Kirsch, S.H., Herrmann, W., Rabagny, Y., and Obeid, R. (2010). Quantification of acetylcholine, choline, betaine, and dimethylglycine in human plasma and urine using stable-isotope dilution ultra performance liquid chromatography-tandem mass spectrometry. Journal of chromatography B, Analytical technologies in the biomedical and life sciences *878*, 3338-3344.

Kitahara, M., Takamine, F., Imamura, T., and Benno, Y. (2000). Assignment of Eubacterium sp. VPI 12708 and related strains with high bile acid 7alpha-dehydroxylating activity to Clostridium scindens and proposal of Clostridium hylemonae sp. nov., isolated from human faeces. International journal of systematic and evolutionary microbiology *50 Pt 3*, 971-978.

Langmead, B., and Salzberg, S.L. (2012). Fast gapped-read alignment with Bowtie 2. Nat Methods *9*, 357-359.

Langmead, B., Trapnell, C., Pop, M., and Salzberg, S.L. (2009). Ultrafast and memory-efficient alignment of short DNA sequences to the human genome. Genome biology *10*, R25.

Qin, J., Li, R., Raes, J., Arumugam, M., Burgdorf, K.S., Manichanh, C., Nielsen, T., Pons, N., Levenez, F., Yamada, T.*, et al.* (2010). A human gut microbial gene catalogue established by metagenomic sequencing. Nature *464*, 59-65.

R Core Team (2012). R: A Language and Environment for Statistical Computing (Vienna, Austria).

Ridlon, J.M., Kang, D.J., and Hylemon, P.B. (2006). Bile salt biotransformations by human intestinal bacteria. Journal of lipid research *47*, 241-259.

Ridlon, J.M., Kang, D.J., and Hylemon, P.B. (2010). Isolation and characterization of a bile acid inducible 7alpha-dehydroxylating operon in Clostridium hylemonae TN271. Anaerobe *16*, 137-146.

Varemo, L., Nielsen, J., and Nookaew, I. (2013). Enriching the gene set analysis of genome-wide data by incorporating directionality of gene expression and combining statistical hypotheses and methods. Nucleic Acids Res *41*, 4378-4391.

Supplemental Figures and Legends
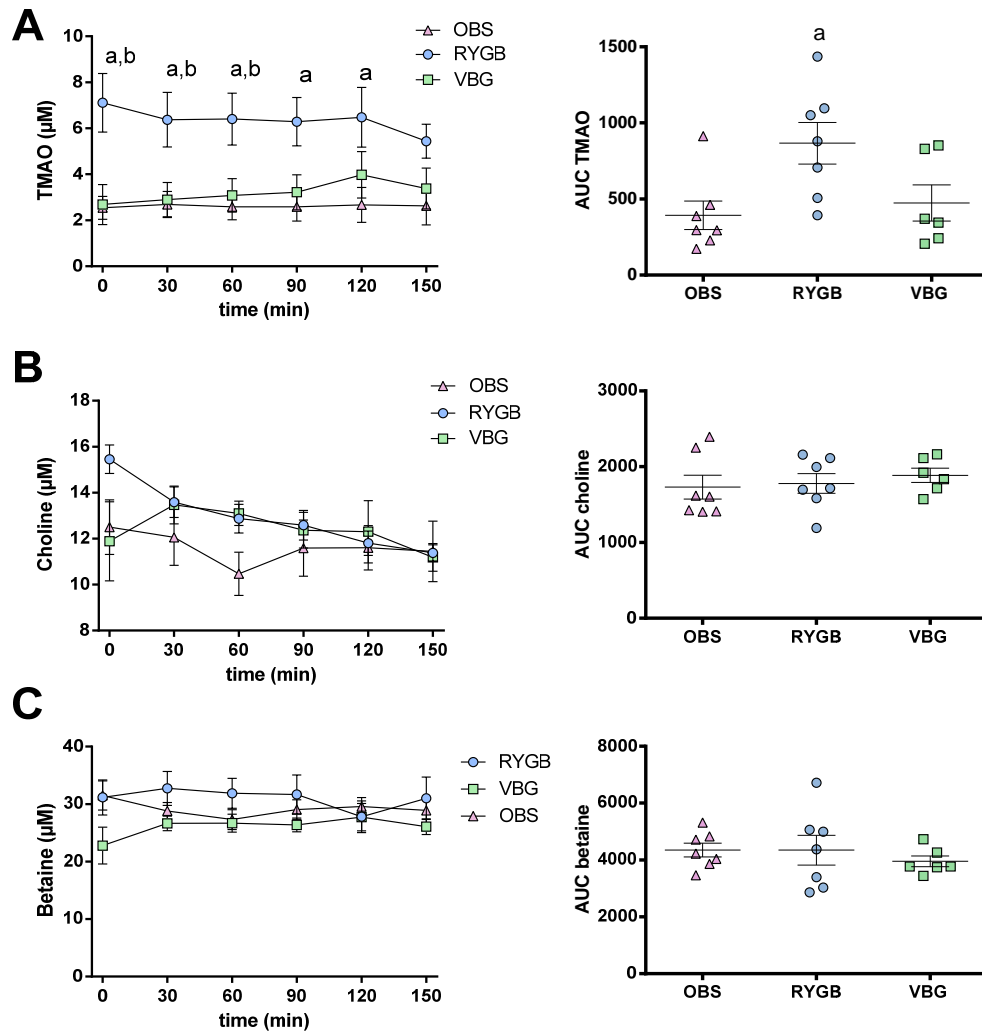
Figure S1. Measurement of TMAO, Choline and Betaine in the Plasma of RYGB, VBG and OBS Women. Related to Figure 2 and Table 1.
(A) Circulating levels of TMAO, (B) choline and (C) betaine. The concentrations of TMAO, choline and betaine were measured during fasting and every 30 minutes for 2.5 hours after a standard meal. Plasma samples for one woman in the VBG group could not be obtained, so the results represent the mean ± standard error of the mean for 7 RYGB, 6 VBG and 7 OBS women. [a] P<0.05 for RYGB compared to OBS and [b] P<0.05 for RYGB compared to VBG according to one-way ANOVA with Tukey's correction for multiple comparisons.
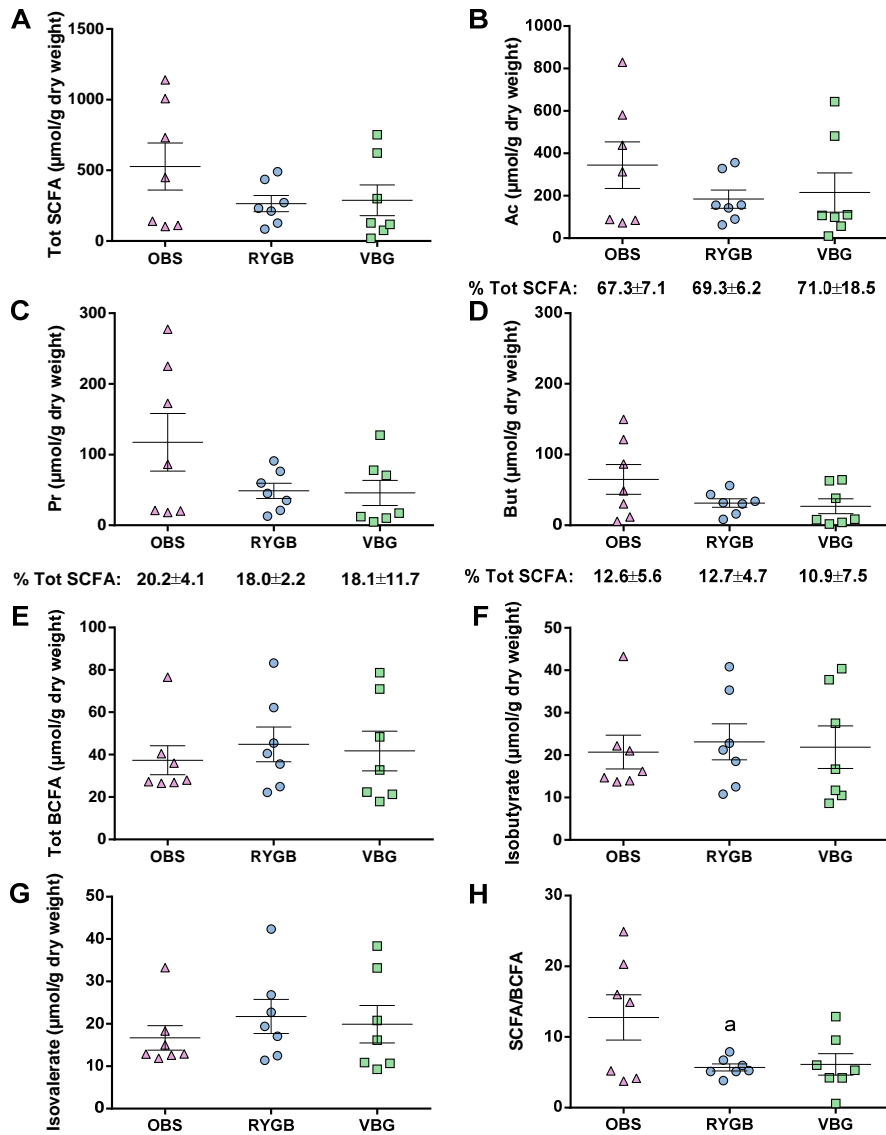
**Figure S2. Measurement of Short-Chain Fatty Acids (SCFAs) and Branched-Chain Fatty Acids (BCFAs) in Stools from the RYGB, VBG and OBS Women. Related to Figure 2.**
(A) Total SCFAs measured as the sum of the concentrations of acetate, propionate and butyrate.
(B) Concentration of acetate (Ac), (C) propionate (Pr) and (D) butyrate (But). The relative proportions of acetate, propionate and butyrate in the total SCFA pools (% Tot SCFA) are indicated under each plot. (E) Total BCFAs measured as the sum of the concentrations of isobutyrate and isovalerate. (F) Concentration of isobutyrate and (G) isovalerate. (H) Ratio of SCFA/BCFA as a measure of microbial fermentation of carbohydrates versus proteins.
Concentrations were normalized to the dry weight of the extracted sample. Results are presented as mean ± standard error of the mean. [a] P<0.05 for RYGB compared to OBS according to one-way ANOVA with Tukey's correction for multiple comparisons.

A

BaiA
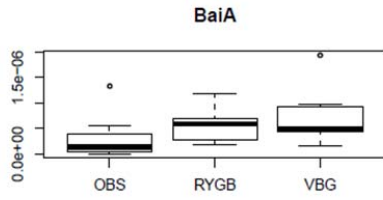
adj. P OvR=0.76 OvV=0.5 RvV=1

BaiB

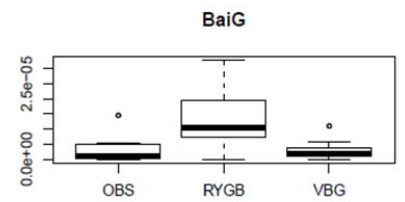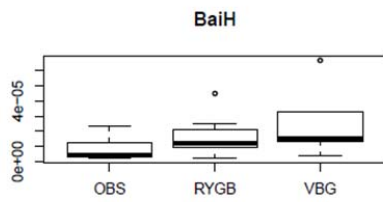adj. P OvR=0.34 OvV=1 RvV=1

BaiCD
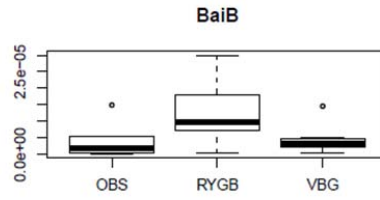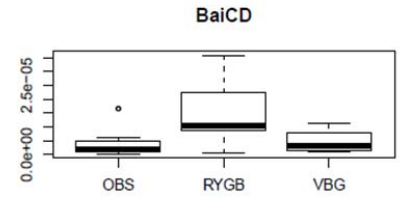
adj. P OvR=0.24 OvV=1 RvV=1
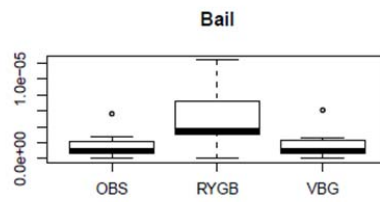
BaiE
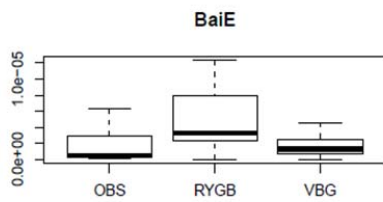
adj. P OvR=0.45 OvV=1 RvV=1
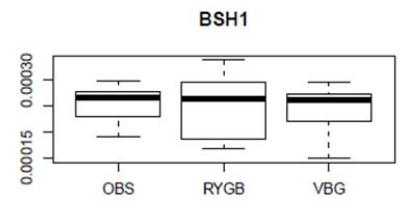
BaiF

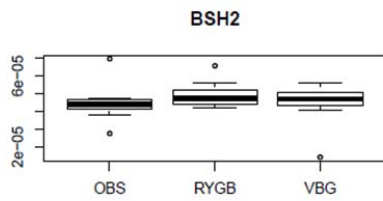adj. P OvR=0.34 OvV=1 RvV=1

BaiG
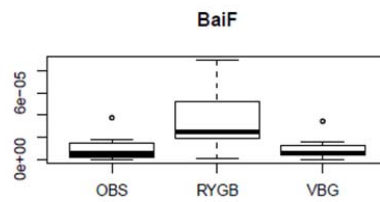
adj. P OvR=0.41 OvV=1 RvV=1

BaiH

adj. P OvR=0.46 OvV=0.12 RvV=1

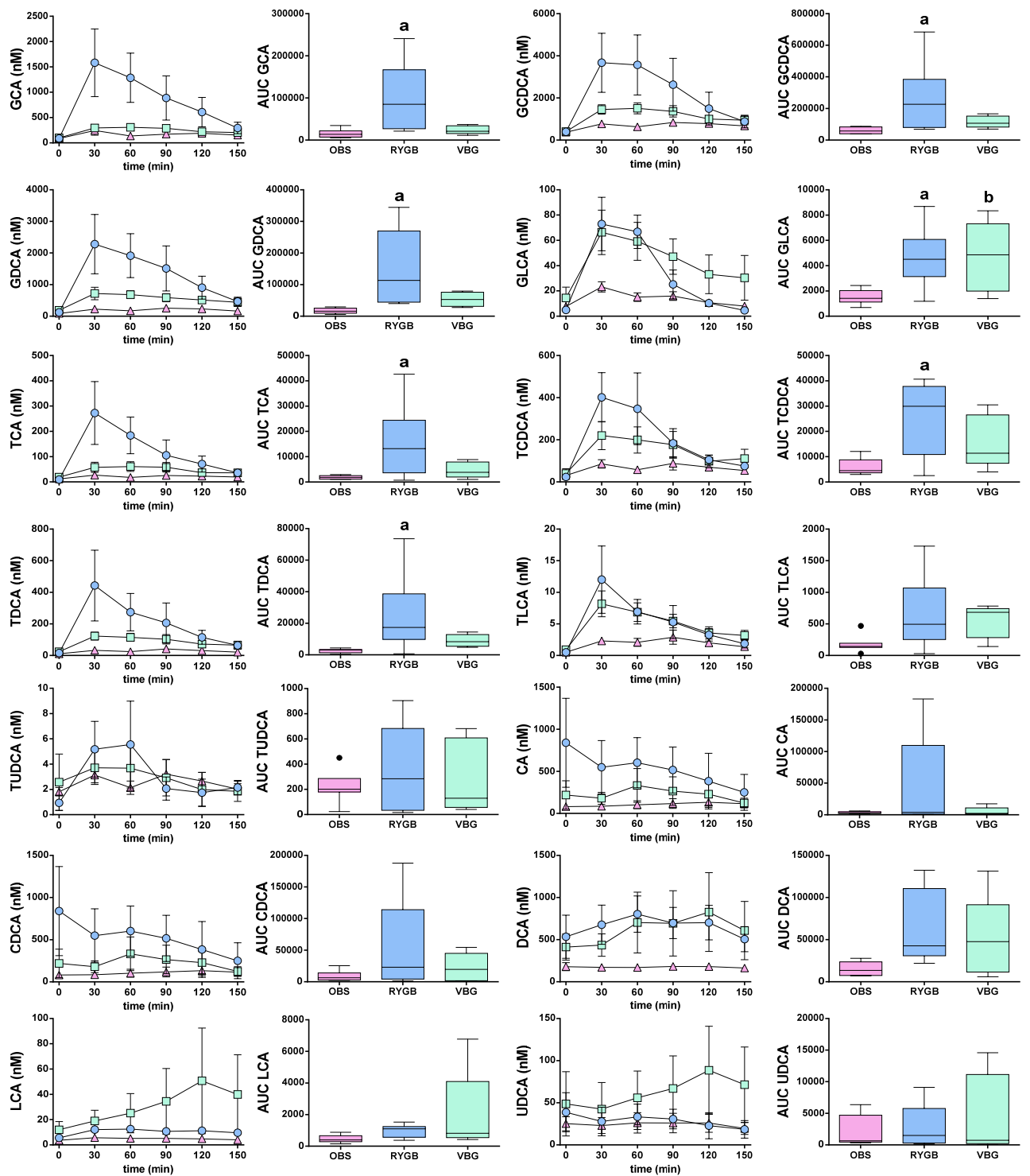BaiI

adj. P OvR=0.44 OvV=1 RvV=1

BSH1

adj. P OvR=0.8 OvV=0.85 RvV=1

BSH2

adj. P OvR=1 OvV=0.95 RvV=1

B

Figure S3. Identification of Microbial Genes for Bile Acid Metabolism and Quantification of Circulating Bile Acids after Bariatric Surgery. Related to Figure 3.

(A) Abundance of putative genes for bile acid metabolism by the gut microbiota. The details about the annotation of *bai* and *bsh* genes are described in Supplemental Experimental Procedures. Boxes denote the interquartile range (IQR) between the first and third quartiles and the line within denotes the median; whiskers denote the lowest and highest values within 1.5 times IQR from the first and third quartiles, respectively. Circles denote data points beyond the whiskers. Adjusted P values for pairwise comparisons between groups are provided under each figure using the initial letter for each group, e.g OvR for OBS vs RYGB. Bai, bile acid-inducible genes; BSH, bile salt hydrolases.

(B) Circulating bile acid concentrations in RYGB, VBG and OBS women. Plasma bile acids concentrations were measured during fasting and every 30 minutes for 2.5 hours after a standard meal. Plasma samples from colecystectomized patients (one in the RYGB and one in the VBG group) were excluded from the analysis, and plasma samples for one VBG woman could not be obtained, so the results represent the mean ± standard error of the mean for 6 RYGB, 5 VBG and 7 OBS women. The Tukey box-plots show the area under the curve (AUC) as a measure of the total postprandial response of each bile acid. [a] P<0.05 for RYGB compared to OBS and [b] P<0.05 for VBG compared to OBS according to one-way ANOVA with Tukey's correction for multiple comparisons. GCA, glycocholic acid; GCDCA, glycochenodeoxycholic acid; GDCA, glycodeoxycholic acid; GLCA, glycolithocholic acid; TCA, taurocholic acid; TCDCA, taurochenodeoxycholic acid; TDCA, taurodeoxycholic acid; TLCA, taurolithocholic acid; TUDCA, tauroursodeoxycholic acid; CA, cholic acid; CDCA, chenodeoxycholic acid; DCA, deoxycholic acid; LCA, lithocholic acid; UDCA, ursodeoxycholic acid.
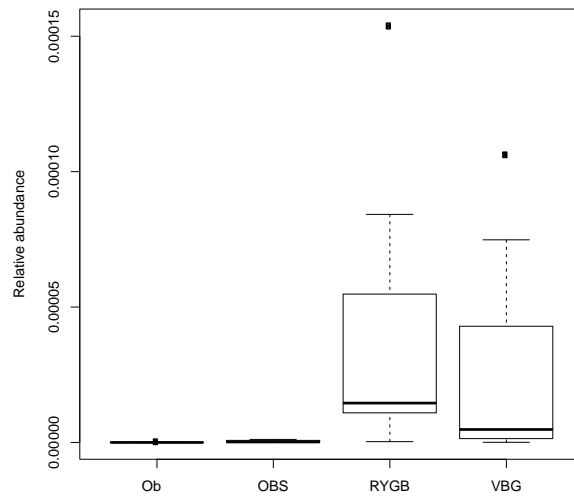
Figure S4. Enrichment of the KO Coding for Trimethylamine *N*-Oxide (TMAO) Reductase. Related to Figure 4 and Table S5.

Relative abundance of the KO coding for the TMAO reductase (K07811) in RYGB, VBG, OBS and Ob women. Boxes denote the interquartile range (IQR) between the first and third quartiles and the line within denotes the median; whiskers denote the lowest and highest values within 1.5 times IQR from the first and third quartiles, respectively. Filled squares denote data points beyond the whiskers.
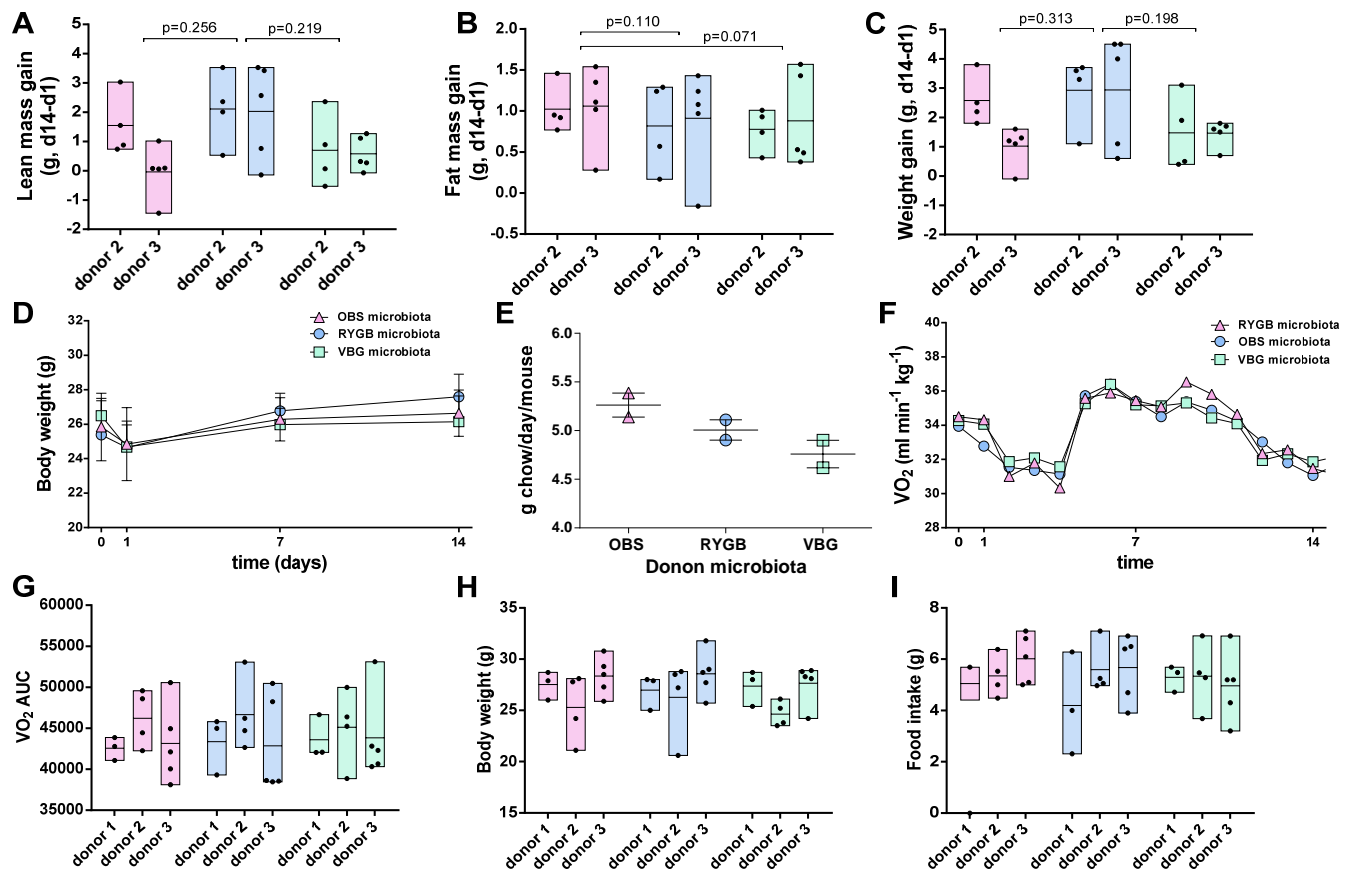
Figure S5. Weight Gain and Metabolism of the Colonized Mice During the Two-Week Colonization Period. Related to Figure 5.

(A) Absolute lean mass gain, (B) absolute fat mass gain and (C) absolute weight gain for mice colonized with fecal microbiota from RYGB, VBG or OBS women. Lean mass, fat mass and weight gains were calculated as the difference between values measured at the end of the experiment (d14) and 1 day after colonization (d1). (D) Body weight and (E) food consumption for mice colonized with fecal microbiota from RYGB, VBG or OBS women. 4-5 mice were colonized *per* donor microbiota for a total of 2 donors in each of the RYGB, VBG and OBS groups.

(F) Oxygen consumption (VO_2) over the 22 h period in the Somedic Chamber and (G) area under the curve (AUC) as a measure of total VO_2. (H) Body weight and (I) food intake for the colonized mice while in the Somedic chamber. Food intake was measured for the total 22 h period in the Somedic chamber. 3-5 mice were colonized *per* donor microbiota for a total of 3 donors in each of the RYGB, VBG and OBS groups.

The lines in the bars indicate mean values of measured parameters in mice colonized with the same donor microbiota. For the curves in panel F, only mean values are shown. The statistical significance of differences between the means was tested by one-way ANOVA with Tukey's correction for multiple comparisons (Panels G-I, Adj. P>0.7, values not shown).